BULLETIN OF THE CHEMICAL SOCIETY OF JAPAN VOL. 42 2801—2807 (1969)

Effects of Cation Vacancies of the Diffusion of Nickel Ions in Defective Spinels

Goro YAMAGUCHI, Mitsuko NAKANO and Mamoru TOSAKI

Department of Industrial Chemistry, Faculty of Engineering, The University of Tokyo, Hongo, Bunkyo-ku, Tokyo

(Received April 7, 1969)

In order to clarify the influence of composition-dependent cation vacancies in defective spinels on the diffusion, the diffusion rates of Ni^{2+} in several kinds of defective spinels ($MgO \cdot xAl_2O_3$, where $x=1.1$, 1.2, 1.3, 1.4 and 1.5) and a perfect spinel ($MgO \cdot Al_2O_3$) were measured by the use of an electron probe micro-analyzer, and the diffusion coefficients were obtained. The diffusion coefficients were found to be linear to the concentrations of the composition-dependent vacancies. The so-called activation energies which were calculated from the Arrhenius plot were about 70 kcal/mol for the defective spinels and 106 kcal/mol for the perfect spinel. It may be concluded that composition-dependent cation vacancies govern the diffusion of cations in the defective spinel, while temperature-dependent vacancies probably predominate in the perfect spinel.

The diffusion in ionic crystals has been well investigated with regard to sodium chloride.[1] It has been shown that there are two ranges in the Arrhenius plot of the self-diffusion coefficients of Na^+ in sodium chloride. This phenomenon may be explained as follows: in the lower temperature range the concentration of the vacancies which are caused by impurities and which govern the diffusion is much larger than that of the temperature-dependent vacancies, while in the higher temperature range the temperature-dependent vacancies predominate. The same phenomenon was found with regard to the self-diffusion of O^{2-} in aluminum oxide,[2] and it is thought that the vacancies caused by impurities contribute to the diffusion in the case of oxide as well.

As for the effect of impurities, the influence of impurities (Fe_2O_3, Cr_2O_3 and CoO) on the diffusion of Ni^{2+} in magnesium oxide has been reported.[3] It was found that when Fe_2O_3 or Cr_2O_3 was added to MgO the diffusion of Ni^{2+} in MgO was promoted. The phenomenon can be explained by the fact that, when Mg^{2+} is replaced with Fe^{3+} or Cr^{3+}, the difference in the valence causes cation vacancies which then contribute to the diffusion.

The no-cation sites in oxide crystals may be classified into the three groups: the structural no-cation sites, the temperature-dependent vacancies, and the composition-dependent vacancies. An example of a structural no-cation site is the no-Al octahedral site in alpha-Al_2O_3. The vacancies caused by impurities belong to the composition-dependent vacancy, and the temperature-dependent vacancy is thermally formed. Composition-dependent vacancies can be intentionally realized and controlled in a complex oxide with a fairly wide solid-solution range such as spinel. Such vacancies caused by structural nonstoichiometry are expected to contribute to the diffusion, but no study of this problem has yet been reported. This paper will report the results of an experiment investigating the influence on the diffusion of cation vacancies occuring in a spinel solid solution.

The $MgAl_2O_4$-Al_2O_3 system has a large region of a

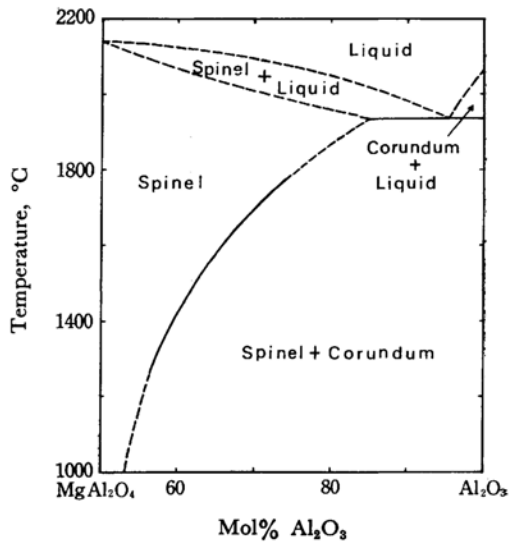

Fig. 1. Phase diagram for the system $MgAl_2O_4$-Al_2O_3.[4]

1) D. Mapother, H. N. Crooks and R. Maurer, *J. Chem. Phys.*, **18**, 1231 (1950).

2) Y. Oishi and W. D. Kingery, *ibid.*, **33**, 480 (1960).

3) G. Yamaguchi and T. Tokuda, *J. Ceram. Assoc. Japan*, **76**, 350 (1968).

solid solution on the side of spinel, as may be observed in the phase diagram[4] (Fig. 1). In this report this solid solution will be called the "defective spinel,"[5] while the spinel with a perfect spinel structure will be called the "perfect spinel." It is thought that excessive oxygen causes cation vacancies with an increase in the Al_2O_3 concentration in the defective spinel[6] and that they are composition-dependent vacancies. Because of the wide range of solubility, the concentration of composition-dependent vacancies can be much larger than that of temperature-dependent defects. Since the concentration gradient was found in the spinel layer at the time of practical formation from magnesium oxide and aluminum oxide,[7] the defective spinel whose composition varies continuously is thought to constitute the product layer. The material transport through the product layer controls the reaction rate in a solid state reaction such as spinel formation. Accordingly, it is important in the study of the solid state reaction to examine the influence on the diffusion of cation vacancies present in the defective spinels.

In this report the diffusion rates of Ni^{2+} in several kinds of defective spinels ($MgO \cdot xAl_2O_3$, where $x=1.1$, 1.2, 1.3, 1.4 and 1.5) and the perfect spinel are investigated using an electron probe micro-analyzer, and the influence on the diffusion of composition-dependent cation vacancies in defective spinels is clarified. Spinels also have many structural no-cation sites, such as no-Al sites in alpha-Al_2O_3; this experiment might be able to suggest the nature of the effect of those no-cation sites on the cation diffusion.

Experimental

Preparation of Specimens. The spinels whose compositions are listed in Table 1 were synthesized from basic magnesium carbonate, basic nickel carbonate, and gibbsite. Ten per cent of the Mg^{2+} of the spinels designated as M1, M2, M3, M4, M5, and M6 were replaced with Ni^{2+}; these spinels were designated as N1, N2, N3, N4, N5, and N6 respectively. The degrees of defectiveness or the concentrations of the composition-dependent cation vacancies of Nj may be expected to be equal to that of Mj, where $j=1$, 2, 3, 4, 5, and 6. The calculated concentrations of such vacancies are shown in Table 1.

Mg^{2+} and Ni^{2+} are similar in valence, ionic radius, and chemical property, and the concentrations of Ni^{2+} in the spinels of the N series are not large. Therefore, the properties of the spinels of the N series are thought to be very similar to those of the M series. Therefore, when M1 and N1, M2 and N2, and so on are paired as

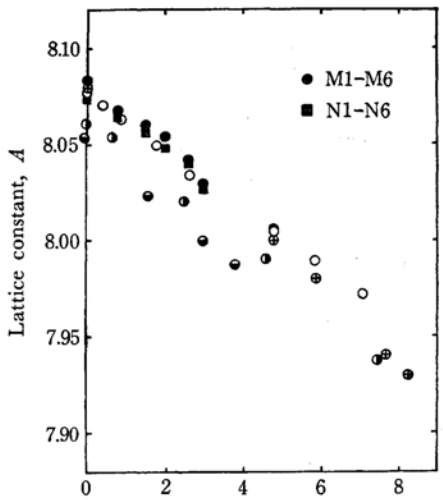

Fig. 2. Lattice constants of spinels *vs.* calculated concentrations of composition-dependent cation vacancies.
● and, ■ this experiment; ○, I. I. Visknerskii and V. N. Skripak; ◑, D. M. Roy, R. Roy and E. F. Osborn; ◐, P. T. Sarjeant and R. Roy; ◒, G. Hägg and G. Söderholm; ⊕, G. Yamaguchi

TABLE 1. COMPOSITIONS OF SPECIMENS AND THE CALCULATED CONCENTRATIONS OF COMPOSITION-DEPENDENT CATION VACANCIES*

Designation	Composition	Designation	Composition	Concn. of cation vacancies (cation site %)
M1	$MgO \cdot Al_2O_3$	N1	$(Mg_{0.9}Ni_{0.1})O \cdot Al_2O_3$	0.0
M2	$MgO \cdot 1.1Al_2O_3$	N2	$(Mg_{0.9}Ni_{0.1})O \cdot 1.1Al_2O_3$	0.78
M3	$MgO \cdot 1.2Al_2O_3$	N3	$(Mg_{0.9}Ni_{0.1})O \cdot 1.2Al_2O_3$	1.45
M4	$MgO \cdot 1.3Al_2O_3$	N4	$(Mg_{0.9}Ni_{0.1})O \cdot 1.3Al_2O_3$	2.04
M5	$MgO \cdot 1.4Al_2O_3$	N5	$(Mg_{0.9}Ni_{0.1})O \cdot 1.4Al_2O_3$	2.57
M6	$MgO \cdot 1.5Al_2O_3$	N6	$(Mg_{0.9}Ni_{0.1})O \cdot 1.5Al_2O_3$	3.03

* Porosities of specimens are within the range of 1 to 3%.

4) D. M. Roy and E. F. Osborn, *J. Am. Ceram. Soc.*, **36**, 147 (1953).
5) G. Yamaguchi, This Bulletin, **26**, 204 (1953).
6) G. Hägg and G. Söderholm, *Z. Physik. Chem.*, **B29**, 88 (1935).
7) G. Yamaguchi and T. Tokuda, This Bulletin, **40**, 843 (1967).

diffusion couples, the degree of defectiveness does not vary at the time of diffusion treatment and Ni^{2+} ions may be expected to diffuse with the same diffusion coefficient on both sides of the diffusion interface. These spinels were pressed into pellets and heated at 1650°C for several hours. Specimens were sintered densely so that they had less than 5% of porosity to avoid its influence as much as possible. The lattice constants of these spinels were measured accurately by an X-ray diffractometer. The measured values are shown in Fig. 2, along with the lattice constants previously reported.[6,8-11] It was found that the lattice constants varied linearly with the compositions in both series, M and N, so that the spinels whose cation-vacancy concentrations are equal to the calculated value may be supposed to have been synthesized. These pellets were polished with silicon carbide grains and diamond paste. Magnesium aluminum spinels were paired with spinels containing Ni^{2+} whose cation-vacancy concentrations were equal to the former, such as M1-N1. Their polished faces were placed in contact, and they were pressed perpendicularly to the contact face under a pressure of about 3 kg/cm² for 15 min at the temperature of 1500°C. After this treatment, the pellets were stuck together.

The specimens prepared as mentioned above were polycrystalline and contained grain boundaries. In order to estimate the influence of grain boundaries on the cation diffusion, two kinds of single crystal spinels were treated in the same way as the sintered specimens. The compositions of these single crystals were $MgO \cdot Al_2O_3$ and $MgO \cdot 1.5Al_2O_3$; they were designated as M1(S) and M6(S) respectively. M1(S) was paired with N1, and M6(S) with N6, and they were jointed in the same way as the other couples.

Heat Treatment for Diffusion. The six couples prepared as described above were heated in a controlled electric furnace for from 48 to 216 hr. The heat-treating temperatures were 1305±10, 1372±10, 1477±10, and 1527±10°C.

Analyzing Method. Each specimen was buried in resin after the heat treatment and cut perpendicularly to the diffusion interface with a diamond cutter. The cut surface was polished carefully with silicon carbide grains and diamond paste, and then coated with beryllium by vacuum spattering in order to get the electric conductivity. Specimens were mounted on the sample holder and analyzed by the electron probe micro-analyzer. At the time of measurement specimens were moved perpendicularly to the diffusion interface at a velocity of 20 μ/min, while the electron beam was fixed; then the intensity profile of the characteristic X-rays of Ni was obtained.

For the standard samples the spinels whose compositions are described as $(Mg_{1-x}Ni_x)O \cdot Al_2O_3$, where x=0.0, 0.01, 0.02, and 0.05, were synthesized. They were sintered, polished, and coated with beryllium in the same way as in the case of diffusion couples. With these standard samples, the intensities of the Ni$K\alpha$ rays were measured by the electron probe micro-analyzer. It was found that the plot of the intensities of the Ni$K\alpha$ rays against the concentrations of Ni^{2+} was almost linear, as is shown in Fig. 3. Therefore, it might be supposed that the intensity profile of Ni$K\alpha$ rays obtained

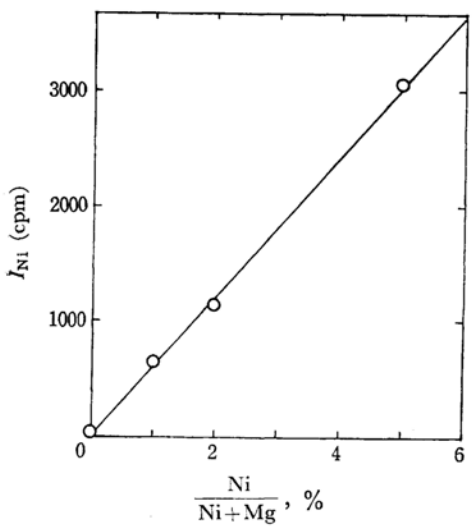

Fig. 3. Plot of Ni$K\alpha$ intensities *vs.* concentrations of Ni^{2+}.

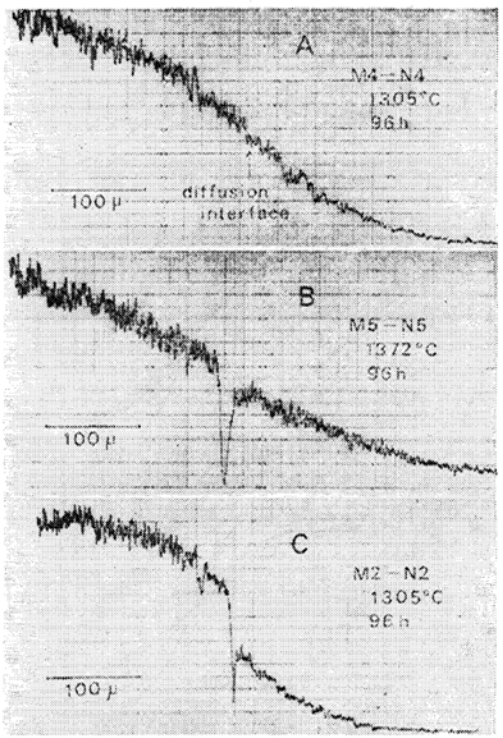

Fig. 4. The typical profiles belonging to the three classes represented by the adhesive sign A, B and C.

8) G. Yamaguchi, *J. Ceram. Assoc. Japan*, **61**, 594 (1953).
9) I. I. Visknerskii and V. N. Shripk, *Soviet Phys.-Solid State*, **7**, 2374 (1966).
10) D. M. Roy, R. Roy and E. F. Osborn, *Am. J. Sci.*, **251**, 337 (1953).
11) P. T. Sarjeant and R. Roy, *J. Appl. Phys.*, **38**, 4540 (1967).

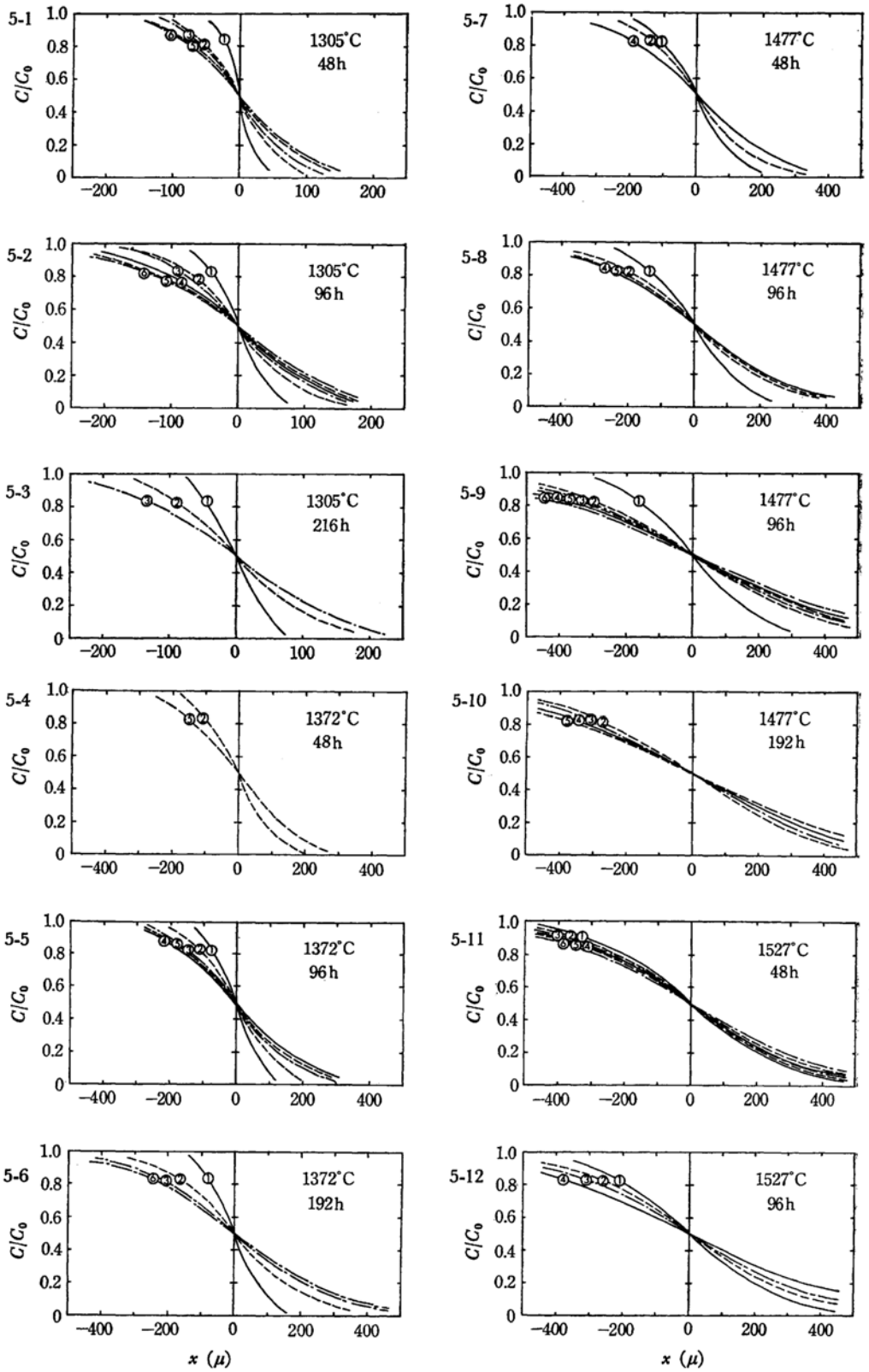

Fig. 5. Concentration distributions of Ni^{63+} in the diffusion couples.
—①—, M1-N1; --②--, M2-N2; —③—, M3-N3; —④—, M4-N4; --⑤--, M5-N5; —⑥—, M6-N6

by the measurement about the diffusion couple represents the concentration distribution of Ni^{2+} as it really is.

Results and Calculation of Diffusion Coefficients

The intensity profiles of Ni$K\alpha$ rays measured by the electron probe micro-analyzer can be grouped into the following three classes on the basis of the features of the diffusion interface and its neighborhood. The first class consists of the profiles which have no clear falling of intensity at the position of the diffusion interface. In the couples of this group the pellets are thought to be stuck very fast; such an adhesive condition is represented by the sign A. The second class consists of the profiles which have clear fallings of intensity at the position of the diffusion interface, but in which the Ni$K\alpha$ intensities on both sides are nearly equal. In this case the pellets are thought to be stuck quite fast; such an adhesive condition is represented by the sign B. The third class consists of the profiles which have clear fallings at the position of the diffusion interface and in which there are gaps of Ni$K\alpha$ intensities on both sides of the diffusion interface. Such an adhesive condition is represented by the sign C. Examples of the original profiles belonging to all three classes recorded by the electron probe micro-analyzer are shown in Fig. 4. The experiments whose results have the profiles represented by the adhesive signs A and B were thought to be established well enough, and so the results were used as data for the calculation of the diffusion coefficients. The results of the experiments belonging to the class represented by the adhesive sign C were not used, however, because in this case the adhesive condition was thought to be not so good.

The intensity profile was smoothed so as to average the statistical fluctuations; it can now be thought of as a smoothed profile to represent the concentration distribution of Ni^{2+} in the diffusion couple as it really is. The concentration distribution curves of Ni^{2+} in the diffusion couples which are thought to be well establsihed are shown in

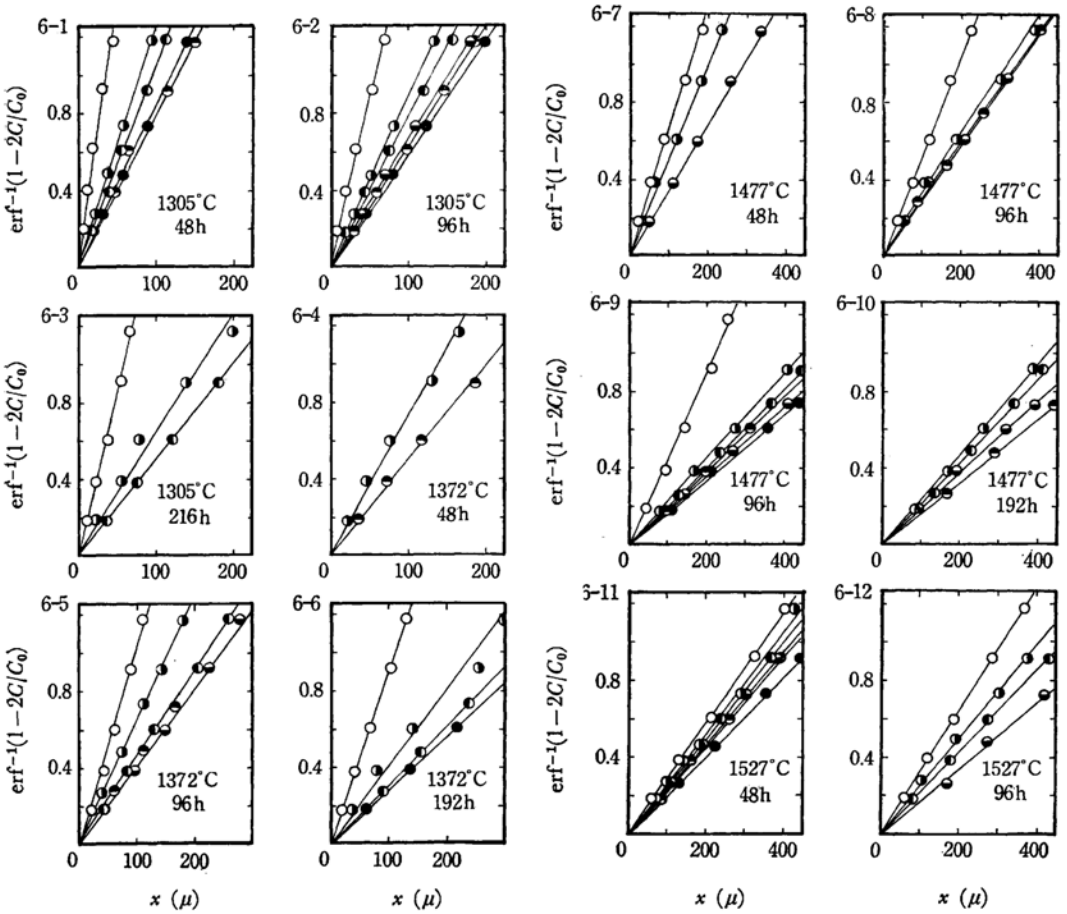

Fig. 6. Plots of $\mathrm{erf}^{-1}(1-2C/C_0)$ *vs.* x.

○, M1-N1; ◑, M2-N2; ◐, M3-N3; ◒, M4-N4; ◓, M5-N5; ●, M6-N6

Figs. 5-1 to 5-12. The shapes of the curves are symmetrical, as is shown in Figs. 5-1 to 5-12; on both sides of the diffusion interface the equal values of the diffusion coefficient of Ni^{2+} were calculated by the method to be described below.

In obtaining the diffusion coefficients, it was assumed that the diffusion follows Fick's law. Considering the initial state, the concentration, C, of Ni^{2+} at a certain distance, x, from the diffusion interface after time t is given by:

$$C = C_0/2 \cdot \{1-\mathrm{erf}(x/2\sqrt{Dt})\}$$

Therfore,

$$\mathrm{erf}^{-1}(1-2C/C_0) = x/2\sqrt{Dt},$$

where D is the diffusion coefficient of Ni^{2+}, C_0 is the initial concentration of Ni^{2+} at $x<0$, $\mathrm{erf}(\xi)$ is Gauss' error function, and $\mathrm{erf}^{-1}(\zeta)$ is the inverse function of Gauss' error function. Plots of $\mathrm{erf}^{-1}(1-2C/C_0)$ against x based on the results shown in Figs. 5-1 to 5-12 are shown in Figs. 6-1 to 6-12. In every plot good straight lines are obtained; from the slope of these lines, that is $1/2\sqrt{Dt}$, the diffusion coefficients can be calculated. The diffusion coefficients of Ni^{2+} obtained in the way described above were arranged for every couple and every heat-treatment temperature; the results are shown in Table 2. In order to estimate the influence of grain boundaries, the diffusion coefficients were calculated from the measurements of M1(S)-N1 and M6(S)-N6; it was found that they were nearly equal to the values obtained from M1-N1 and M6-N6 respectively. The plots of $\mathrm{erf}^{-1}(1-2C/C_0)$ *vs.* x for M1(S)-N1 and M6(S)-N6 are shown in Fig. 7, along with the plots about M1-N1 and M6-N6. Accordingly, it seems that there is no influence of grain boundaries on the diffusion in such an experiment using a sintered specimen fired at a temperature above 1650°C.

TABLE 2. DIFFUSION COEFFICIENTS OF Ni^{2+} IN DEFECTIVE SPINELS

Couple of specimens	$D\times10^{10}$ (cm²/sec)			
	1305°C	1372°C	1477°C	1527°C
M1-N1	0.16±0.07	0.63±0.16	3.6±0.5	12±3
M2-N2	0.77±0.15	2.0±0.7	8.2±4.5	15±3
M3-N3	1.2±0.2	3.2±0.9	12±5	18±2
M4-N4	1.6±0.5	3.6±1.2	14±5	24±5
M5-N5	2.0±0.4	4.1±1.3	16±4	26±7
M6-N6	2.2±0.3	5.1±1.0	21±4	32±8

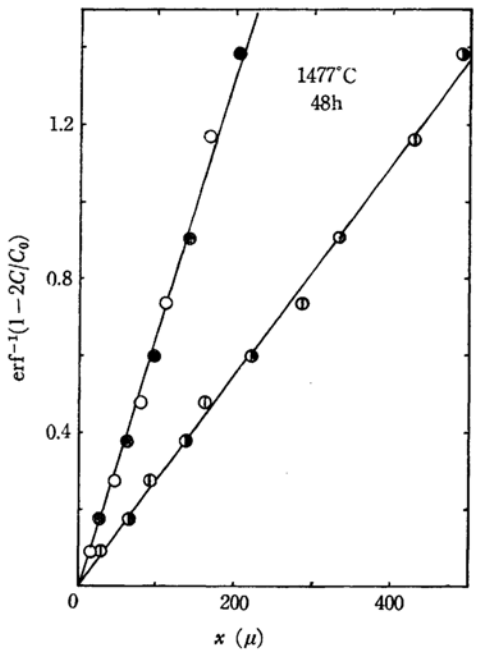

Fig. 7. The plot of $\mathrm{erf}^{-1}(1-2C/C_0)$ *vs.* x about M1-N1, M1(S)-N1, M6-N6 and M6(S)-N6.
○, M1-N1; ●, M1(S)-N1; ⓘ, M6-N6; ◑, M6(S)-N6

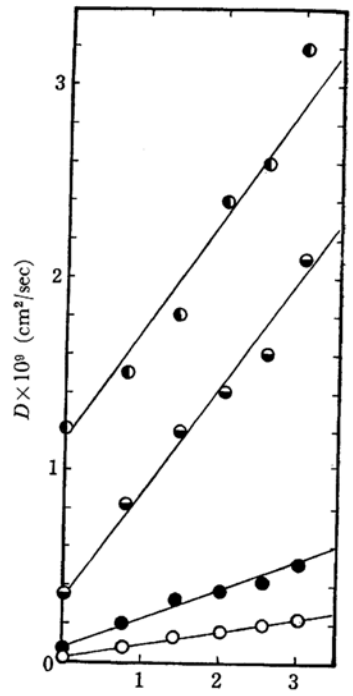

Fig. 8. Plots of diffusion coefficients *vs.* concn. of composition-dependent cation vacancies.
◐, 1527°C; ◒, 1477°C; ●, 1372°C; ○, 1305°C

Discussion

The plots of the diffusion coefficients of Ni^{2+} *vs.* the concentrations of the composition-dependent vacancies are shown in Fig. 8. The figure shows that the diffusion coefficients of Ni^{2+} are linear to

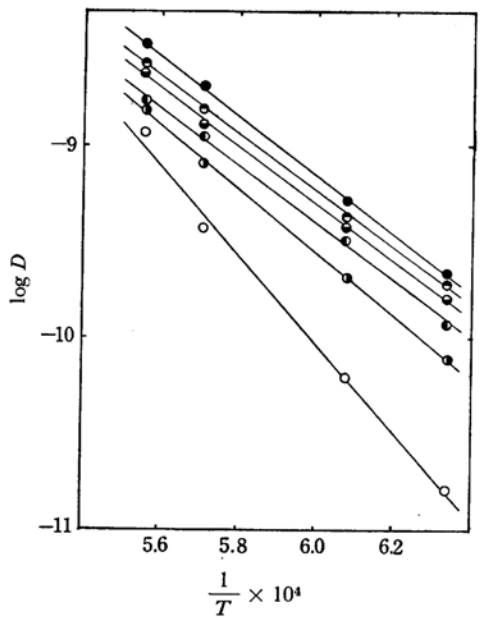

Fig. 9. Arrhenius plot of the diffusion coefficient.
○, M1-N1; ◑, M2-N2; ◐, M3-N3;
◒, M4-N4; ◓, M5-N5; ●, M6-N6

the concentrations of the composition-dependent vacancy. The Arrhenius plot for each couple is shown in Fig. 9. The so-called activation energies obtained from the Arrhenius plots are listed in Table 3. The activation energy is 106 kcal/mol for the M1-N1 couple with a perfect spinel structure, while it is about 70 kcal/mol for the couples containing composition-dependent vacancies, M2-N2, M3-N3, M4-N4, M5-N5, and M6-N6. Therefore, it was confirmed that the composition-dependent vacancies contribute to the cation diffusion in the defective spinel. In the perfect spinel the temperature-dependent vacancy or the structural no-cation site is thought to contribute to the cation diffusion. The fact that the diffusion

Table 3. The temperature dependence of the diffusion coefficients
(the so-called activation energy)

Couple of specimens	So-called activation energy (kcal/mol)
M1-N1	106
M2-N2	75
M3-N3	69
M4-N4	68
M5-N5	67
M6-N6	69

constants of Ni^{2+} in the perfect spinel are fairly small compared with the values in the defective spinels suggests that, if there exists a diffusion caused by the structural no-cation sites, the contribution of those no-cation sites to the diffusion will seem small. However, the effects of the temperature-dependent vacancies and the strucutral no-cation sites could not be discriminated in this experiment. Therefore, according to the genral interpretation, it was assumed that the diffusion in the perfect spinel was caused by the temperature-dependent vacancies. The diffusion coefficient D in M1-N1 can, then, be represented as follows:

$$D = D_0 \exp\left(-\frac{U+E}{RT}\right)$$

where U is the energy necessary for the movement of Ni^{2+} and where E is the energy necessary to form the temperature-dependent vacancy contributing to the diffusion. The so-called activation energy for the perfect spinel, $U+E$, is 106 kcal/mol, as is shown in Table 3. In defective spinels the diffusion coefficient, D, is represented as follows:

$$D = D_0' \exp\left(-\frac{U}{RT}\right)$$

where U is the energy necessary for the movement of Ni^{2+}. The so-called activation energy is about 70 kcal/mol for the defective spinel, as is shown in Table 3. Therefore, the tentative values of $U=70$ kcal/mol and $E=36$ kcal/mol were obtained. This value of E is about 1.6 times larger than the value reported for Na^+ in NaCl, that is, 23 kcal/mol,[1] this ratio does not seem unreasonable. In the case of the diffusion of Ni^{2+} in MgO containing Cr_2O_3, 70 kcal/mol was obtained as the extrinsic activation energy;[3] this is almost equal to the value found in the present investigation.

Conclusion

The diffusion of Ni^{2+} in several kinds of defective spinels and the perfect spinel were investigated using an electron probe micro-analyzer. It was found that the diffusion coefficient of Ni^{2+} in the defective spinel increased linearly with the increase in the concentration of the composition-dependent cation vacancies. The so-called activation energy calculated from the Arrhenius plot for the defective spinel was different from that for the perfect spinel; the difference between them was 36 kcal/mol. The results support the suggestions that the composition-dependent cation vacancies govern the cation diffusion in the defective spinel, while the temperature-dependent vacancies predominate in the perfect spinel.